

Supplementary information for

Characterization of polymeric nanoparticles using analytical ultracentrifugation

Leosveys Diaz, Caroline Peyrot and Kevin J. Wilkinson*

Department of Chemistry, Biophysical Environmental Chemistry group, University of Montreal,
C.P. 6128, succursale Centre-ville, Montreal (QC), Canada H3C 3J7

*Corresponding author: Phone: +1-514 343 6741; fax: +1-514 343 7586; e-mail:
kj.wilkinson@umontreal.ca

Table of contents

S1. Sizes of standard nanoparticles	Page S2
Table S1. Nominal and measured particle diameters	Page S2
Figure S1. Raw sedimentation profiles	Page S3
Figure S2. Hydrodynamic diameters of the nanoparticles	Page S4
Figure S3. Hydrodynamic diameter of the nAg	Page S5
Figure S4. Hydrodynamic diameters of two fluorescent nPS	Page S6
Table S2. Hydrodynamic diameters of two fluorescent nPS	Page S6
S2. Limits to the sensitivity of the AUC detectors	Page S6
Table S3. Hydrodynamic diameters of different concentrations of the allospheres	Page S7
Figure S5. Sedimentation coefficients of different concentrations of the allospheres	Page S7
Figure S6. Hydrodynamic diameter of the allospheres (fluorescence)	Page S8
Figure S7. Raw ultracentrifugation data (allospheres)	Page S9
S3. Comparison of sizes obtained by DLS and AUC	Page S9
Figure S8. Hydrodynamic diameters (allospheres) for different pH	Page S10
Figure S9. Hydrodynamic diameters (allospheres) using DLS	Page S11
Figure S10. Hydrodynamic diameter (allosphere) using AUC	Page S11
Figure S11. Hydrodynamic diameter (allospheres) determined at 40000 rpm (5 mg L ⁻¹)	Page S12
Figure S12. Hydrodynamic diameter (allospheres) determined at 5000 rpm	Page S12
Figure S13. Hydrodynamic diameter (allospheres) determined at 40000 rpm (200 mg L ⁻¹)	Page S13
S4. Size of the soil humic acid (fluorescence correlation spectroscopy)	Page S13
Figure S14. Autocorrelation curve for the FCS	Page S14
S5. Composition of the natural water samples	Page S14
Table S4. Major ions in the natural waters	Page S15
Bibliography	Page S15

S1. Sizes of standard nanomaterials

Nanomaterials (NM) with known sizes were analysed by sedimentation velocity analytical ultracentrifugation (SV-AUC) at 20 °C. Interference detection optics were used to measure nAg, nTiO₂, nZnO, nPS (NIST-52 nm); absorbance detection (wavelength 420 nm) was used for the nAg, and fluorescence detection (excitation: 488 nm; emission: 505 nm) was used for nPS (NIST-24 nm, NIST-54 nm). Centerpieces were filled with 400 µL of the nanoparticles in buffered solutions (10⁻³ M HEPES at pH 7.0; 10⁻³ M MES at pH 6.0). Rotation speeds (5000-40000 rpm corresponding to relative centrifugal forces, RCF of 2016-129024 x g), number of scans and the ultracentrifugation duration were systematically tested, depending on the nature of the nanoparticles. NM concentrations were varied between 5 and 1000 mg L⁻¹. All AUC data were analyzed by the SEDFIT program (version 14.1) in order to determine sedimentation coefficients, which were then transformed into hydrodynamic diameters (d_H). The analysis of the sedimentation velocity profiles obtained with interference optics was performed on the basis of non-interacting species.

For 1 g L⁻¹ of the 54 nm nPS, sedimentation profiles were accumulated at 20000 rpm (32256 x g) for 100 consecutive scans taken at time intervals of 2.40 seconds (Fig. S1A). The most important feature of the sedimentation profiles are the observed sigmoidal shape that migrated with time and as a function of increasing distance from the center of rotation. Using a relative friction coefficient, f/f_0 , of 1.2 (1, 2), which corresponds to a nearly spherical particle, it was possible to identify a single peak corresponding to a sedimentation coefficient of 72.7 S or a diameter of 50.3 ± 7.9 nm (Fig. S1B). The sedimentation coefficient was determined from the position of the peak maxima, whereas the uncertainty was calculated from replicate measurements obtained on different days. Sizes were obtained in a similar manner for the nTiO₂, nAg, nZnO and other nPS (Table S1, Fig. S2, S3, S4). In most cases, a single peak was identified with a hydrodynamic diameter that was very close to the manufacturer's value.

Table S1. Nominal and measured particle diameters determined for several aqueous suspensions of nanoparticles (nTiO₂, nAg, nZnO, nPS). Ultracentrifugation velocity was varied between 10000 (8064 x g) and 40000 rpm (129024 x g), depending on the characteristics (expected diameter, density) of each nanoparticle.

Nanoparticle	Nominal diameter (nm)	Measured diameter (nm)	Ultracentrifugation velocity (rpm)	Particle density (kg m ⁻³)
nTiO ₂	5	3.9 ± 1.4	30000	3900
nAg	1-10	3.6 ± 1.6	10000	3490*
nZnO	20	22.7 ± 2.3	10000	5600
nPS	24	29.6 ± 7.5	30000	1050
nPS	52	49.0 ± 7.2	20000	1050
nPS	54	50.3 ± 7.9	20000	1050

* for the nAg, particle density was determined by taking into account the polymer coating (67% of the particle mass).

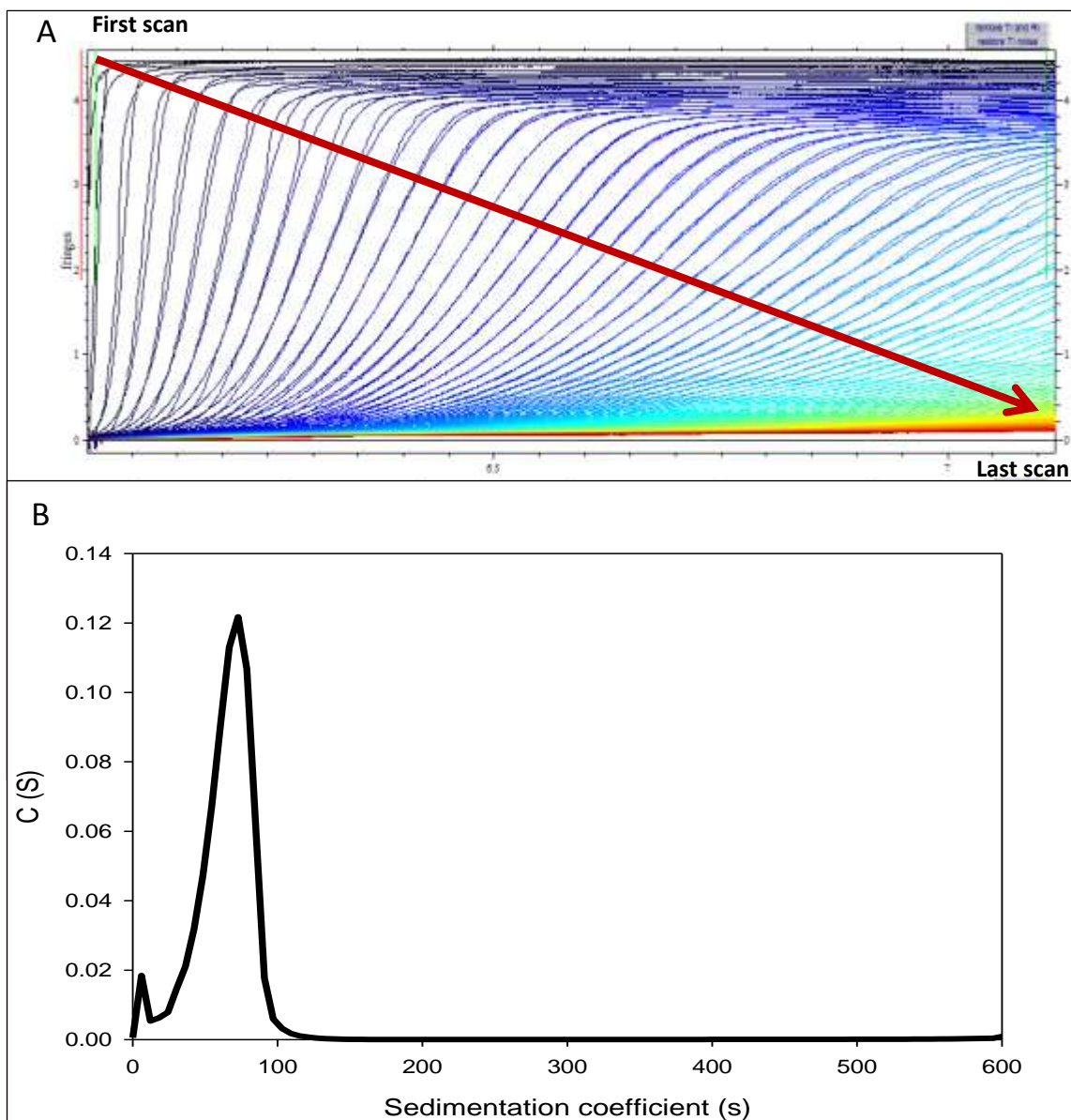
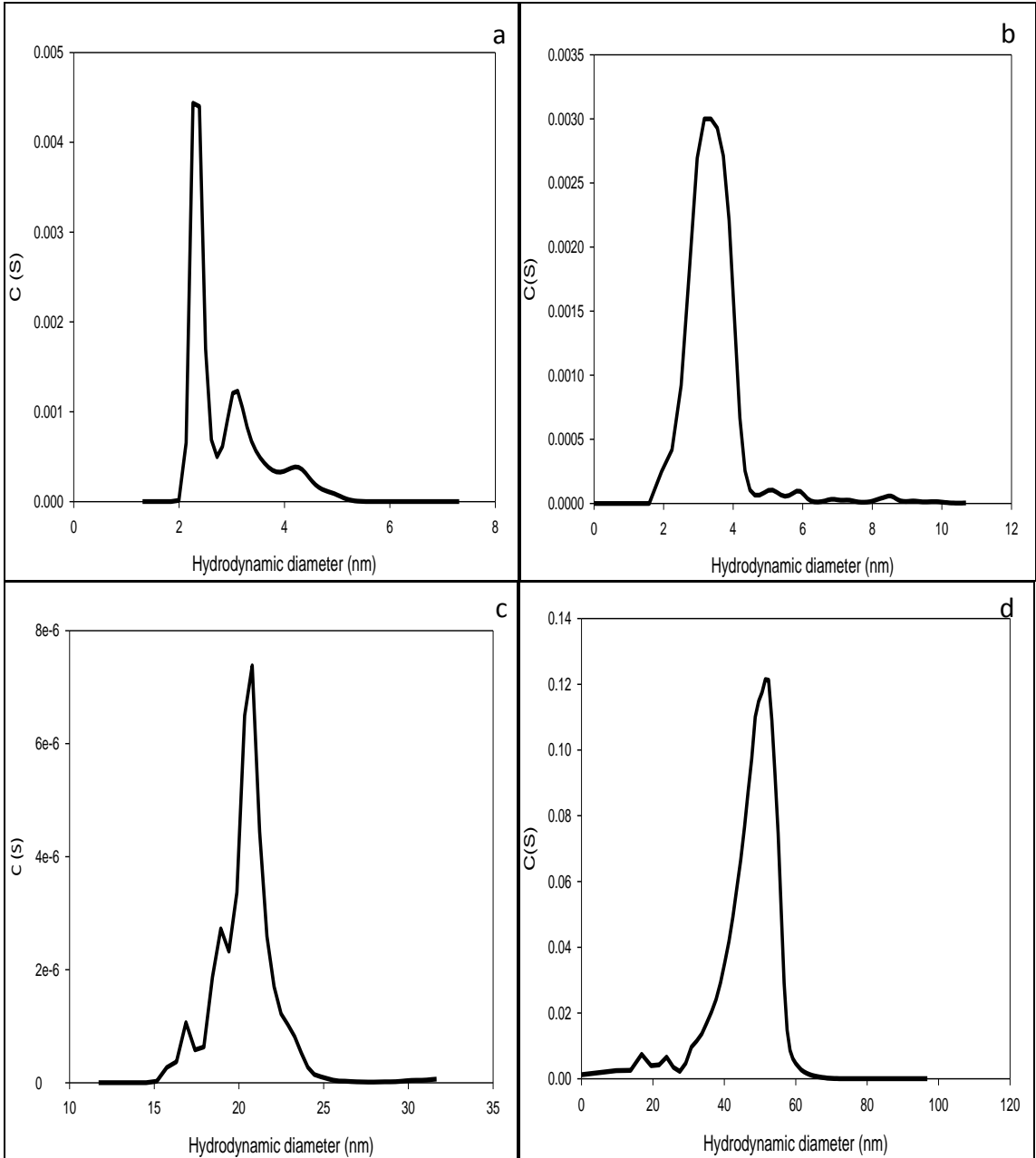


Figure S1A. Raw sedimentation profiles (100 scans) for 1 g L^{-1} of a nPS standard (54 nm) in water when measured using interference optics following centrifugation at 20000 rpm. The x-axis label corresponds to the distance from the center of rotation of the ultracentrifuge. S1B. Sedimentation coefficient distribution (peak maximum at 72.7 S) obtained from the analysis of Figure S1A. All data were acquired using the OPTIMA XL-I (Beckman Coulter). For a particle density of $\rho=1.09 \text{ g cm}^{-3}$ relative to water ($\rho_0=0.997 \text{ g cm}^{-3}$), the sedimentation coefficient corresponded to a particle size of $50.3 \pm 7.9 \text{ nm}$ at the maximum peak intensity.



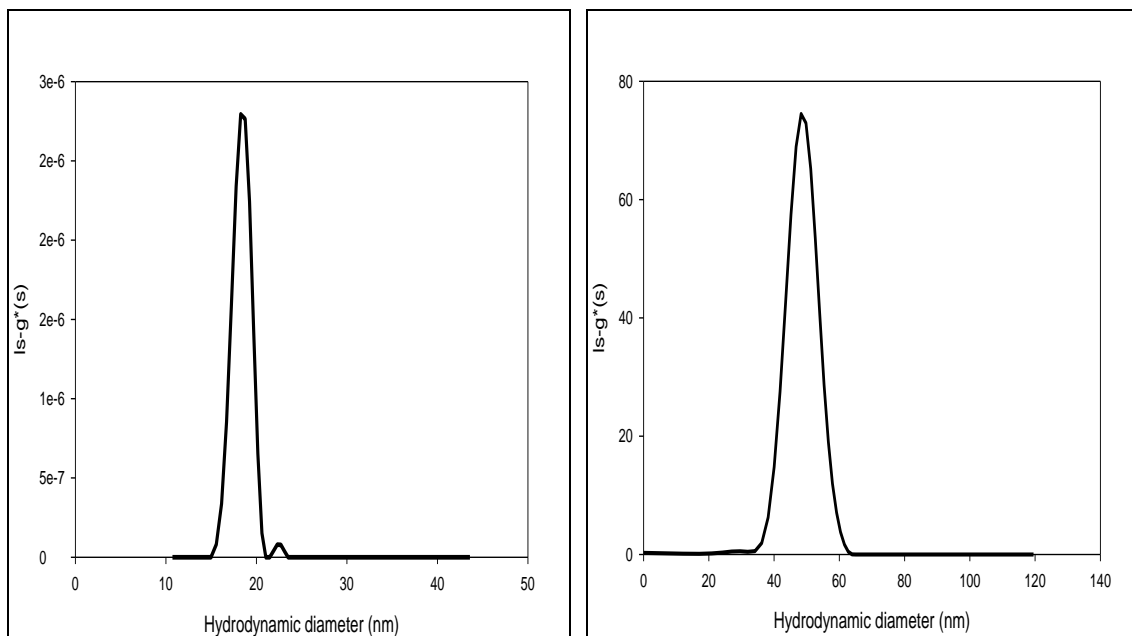


Figure S2. Hydrodynamic diameters of nanoparticles determined by SV-AUC using an interference detector (a) nAg (Vive Nano, nominal diameter of 1-10 nm); (b) nTiO₂ (Nanostructured & Amorphous Material Inc., nominal diameter of 5 nm); (c) nZnO (Nanostructured & Amorphous Material Inc., nominal diameter of 20 nm); (d) nPS (Bangs Laboratories, nominal diameter of 52 nm); (e) nZnO (Nanostructured & Amorphous Material Inc., nominal diameter of 20 nm) and (f) nPS (Bangs Laboratories, nominal diameter of 52 nm). For the two largest particles (e, f), data were determined using a different model (g(s)) as compared to Fig. S2a, b, c, d (c(s) model). Measured sizes are compiled in Table S1.

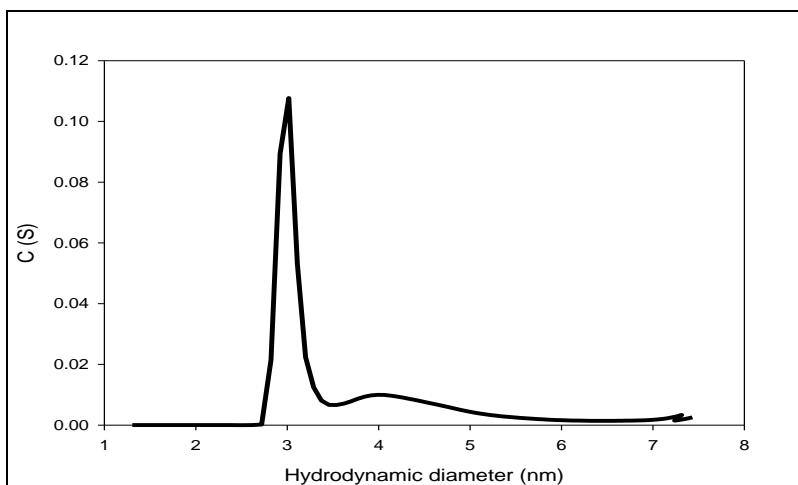


Figure S3. Hydrodynamic diameter of the nAg as determined by SV-AUC using an absorbance detector.

For the nAg, the absorbance detector (420 nm) was also employed (Figure S3) for comparison with the results obtained by interference (Figure S2a). The observed d_H of 3.9 ± 1.2 nm for the nAg corresponded well to that obtained by interference (3.6 ± 1.6 nm) and with previously published literature values (fluorescence correlation spectroscopy: 2.0 ± 0.4 nm; transmission

electron microscopy: 2.0 -10.0 nm (3). Similarly, the labelled nPS could be also be measured using fluorescence detection (Table S2; Figure S4).

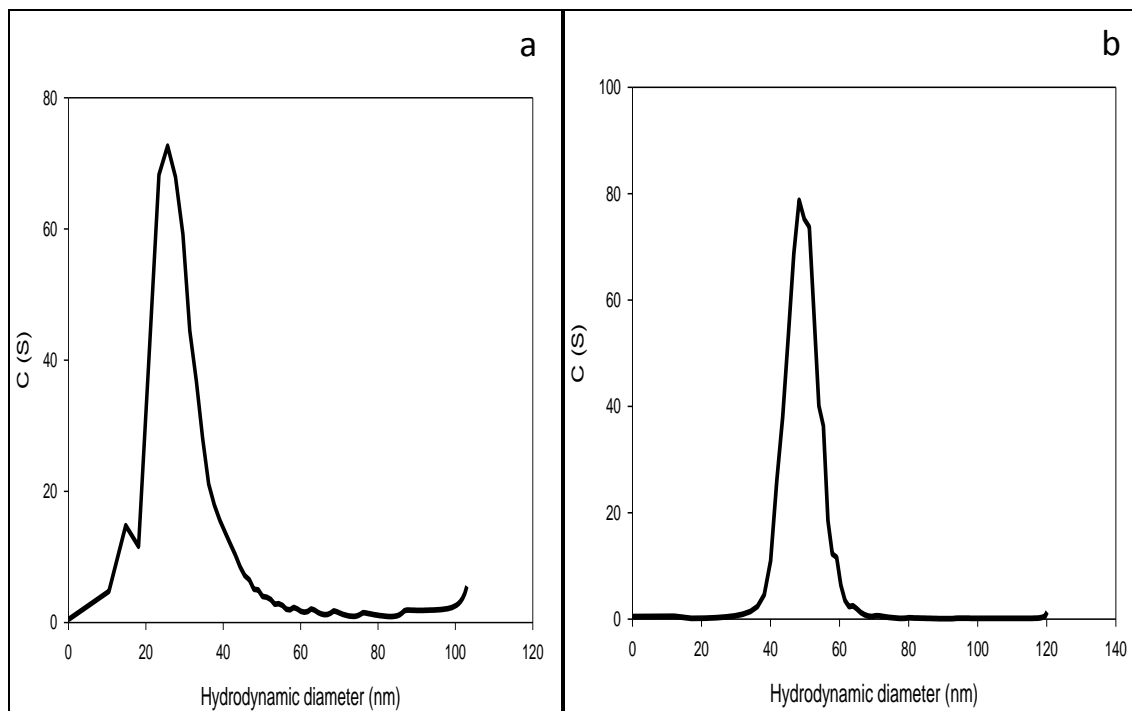


Figure S4. Hydrodynamic diameters of two fluorescent nPS as measured by SV-AUC using fluorescence detection: (a) nPS ((Bangs Laboratories, manufacturer’s diameter 24 nm); (b) nPS ((Bangs Laboratories, manufacturer’s diameter 52 nm). Measured sizes are compiled in Table S2.

Table S2. Hydrodynamic diameters of two fluorescent NM obtained by SV-AUC using a fluorescence detector.

NM	Concentration (mg L ⁻¹)	Nominal diameter (nm)	AUC hydrodynamic diameter (nm)	Ultracentrifugation velocity (rpm)
nPS	1000	24	29.6 ± 7.5	30000
nPS	1000	52	49.0 ± 7.2	20000

A number of preliminary experiments were also performed in order to optimize the ultracentrifugation speed, ultracentrifugation time and number of scans for the size determination of the allospheres. In summary, centrifugal force was important for determining the size of the smaller nanoparticles and better results were obtained at higher speeds, however, slower speeds were necessary to probe agglomeration.

S2. Limits to the sensitivity of the AUC detectors

Based upon the optimization, all subsequent data for the allospheres were acquired at either 5000 rotations per minute (2016 x g) or 40000 rotations per minute (129024 x g) using 400 μL of a pH buffered solution at a sample concentration of 5 mg L⁻¹.

The ability of the AUC to detect low concentrations of the allospheres was evaluated. Since the goal was to examine the most environmentally relevant concentrations of the nanomaterials and based upon preliminary results, the sensitivity study was focused on concentrations ranging between 1 and 5 mg L⁻¹. Particle size distributions could be detected for all 5 concentrations. Some variation was observed among the different concentrations; however, the variability was on a similar order of magnitude as the variation that was observed among replicate samples (± 1.0 nm). Although the allospheres could be detected at all concentrations, the distributions were more reproducible and easier to model for the two highest concentrations (Table S3, Figure S5).

Table S3. Hydrodynamic diameters of different concentrations (1-5 mg L⁻¹) of the polymeric nanoparticles (allospheres) using SV-AUC with interference detection at 40000 rpm.

Concentration (mg L ⁻¹)	AUC hydrodynamic diameter (nm)
1	7.0 \pm 1.7
2	6.9 \pm 1.6
3	7.0 \pm 2.5
4	7.1 \pm 2.3
5	7.0 \pm 2.6

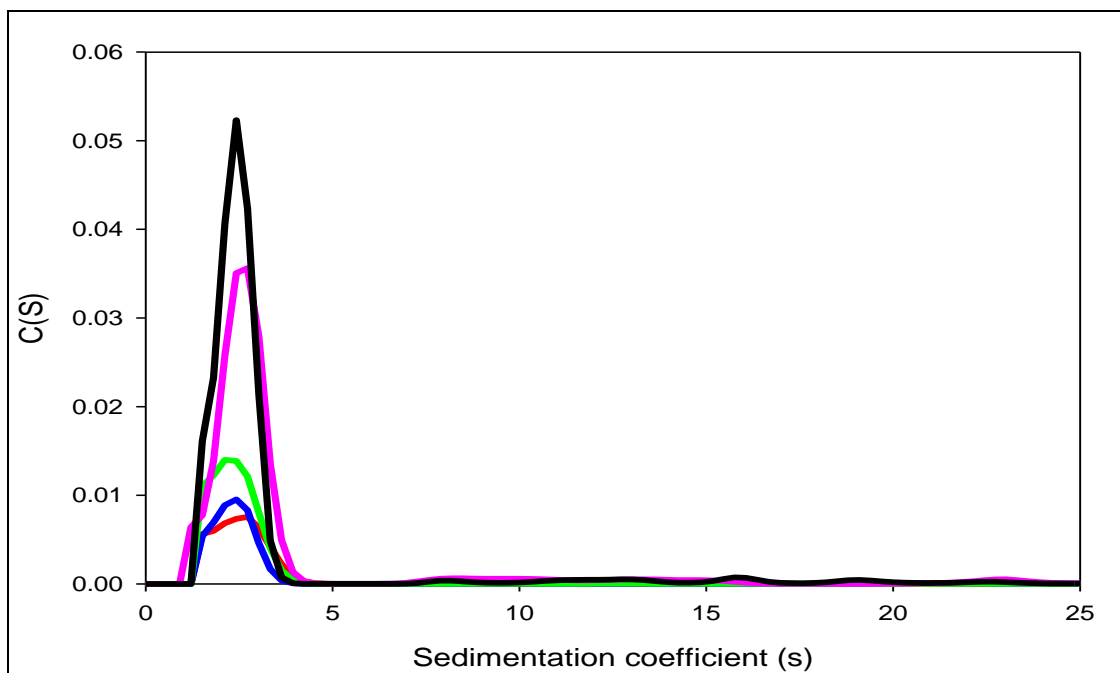


Figure S5. Sedimentation coefficients (S) of different concentrations (1-5 mg L⁻¹) of the polymeric nanoparticles (allospheres) as measured by SV-AUC using interference detection at 40000 rpm. Red line corresponds to 1 mg L⁻¹, blue line to 2 mg L⁻¹, green line to 3 mg L⁻¹, pink line to 4 mg L⁻¹ and black line to 5 mg L⁻¹.

In order to decrease the detectable concentrations further, it would be necessary to improve the sensitivity of detection. Although the bare allospheres do not absorb light, it is possible to add a fluorophore to their structure, either by encapsulation (Nile red) or via adsorption (Rhodamine RG6, Rhodamine 110 and Rhodamine 123) (4). Although a similar particle size was indeed observed following the adsorption of a small amount of 7.6 ± 1.4 nm (Figure S6), surprisingly, no gain in sensitivity was attained. For the Nile Red encapsulated allospheres, similar diameters were obtained using absorbance detection but fluorescence (excitation =488 nm) was below detection limits of the instrument. Accordingly, given that the interference detector did not require the addition of a potentially perturbing fluorophore, the remainder of the experiments were performed using interference optics.

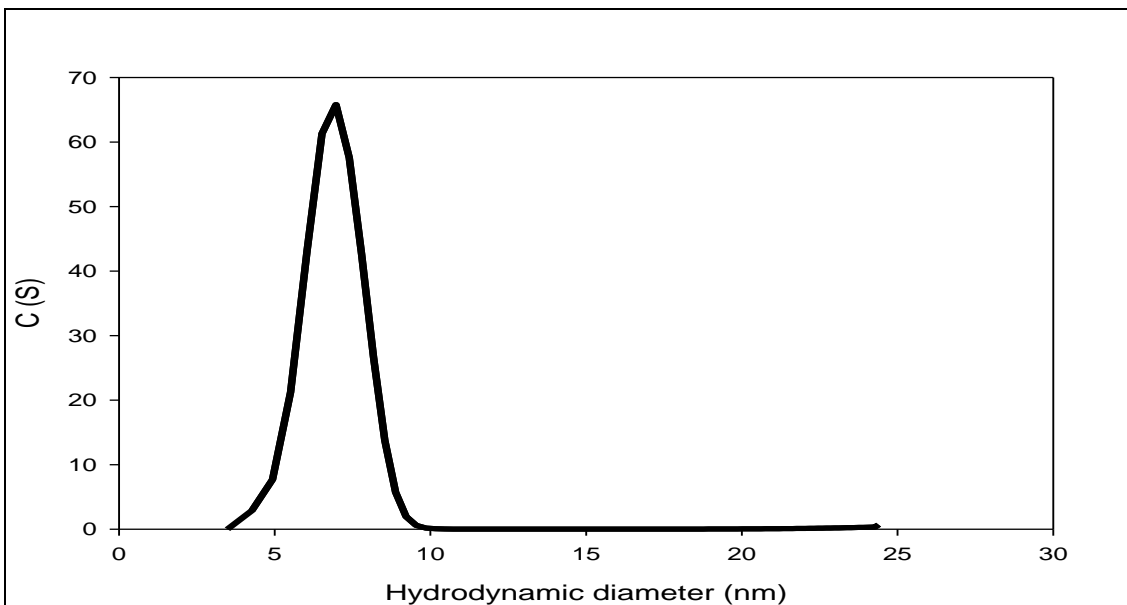


Figure S6. Hydrodynamic diameter of the allospheres (5 mg L^{-1}) obtained by adding 10^{-7} M of rhodamine 123 to the allospheres prior to their measurement by SV-AUC using fluorescence detection.

For 5 mg L^{-1} of the allospheres, the raw data corresponding to interference detection of Figure S6 is presented in Fig. S7.

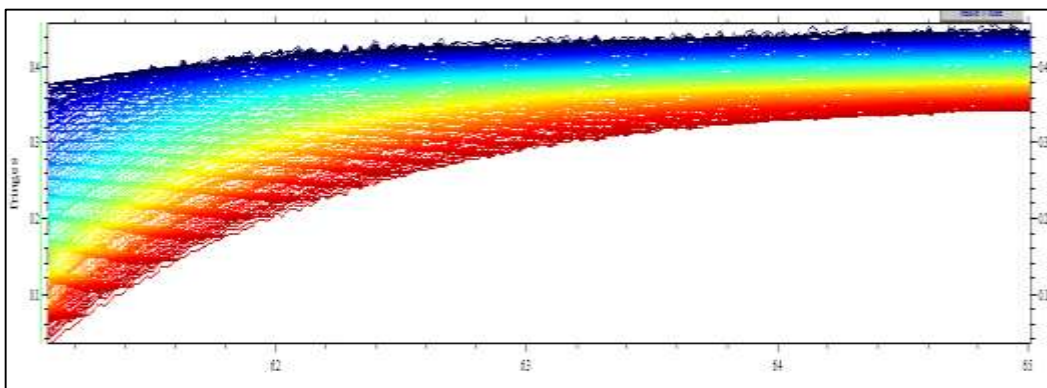


Figure S7. Raw data of fringes vs. position in the centrifugation cell for 5 mg L⁻¹ of the allospheres (pH 6.0)

S3. Comparison of allosphere sizes obtained by DLS and AUC- role of particle concentration

Particle size distributions of the allospheres were determined using both dynamic light scattering (DLS) and AUC at five pH (4.0, 5.0, 6.0, 7.0 and 8.0) (Figure 1, Figures S8 and S9). For 5 mg L⁻¹ of the allospheres, AUC measurements were fairly straightforward (Figure S8), showing particle diameters that varied little with pH. On the other hand, there was not sufficient scattering by the allospheres at 5 mg L⁻¹ to perform DLS experiments and thus concentrations were increased to 200 mg L⁻¹. At the higher concentration, two peaks were observed at pH 7.0 and 8.0: one with a number average diameter of 8.3 ± 0.9 nm corresponding to the monomer and the other at much larger sizes (ca. 185 nm, Figure S9). At the lower pH values (4.0, 5.0, 6.0), agglomeration/sedimentation was so important that suspended particle concentrations decreased below DLS detection limits. On the other hand, the larger agglomerates could be observed by AUC when centrifuging at very low speeds. For example, for 5 mg L⁻¹ of the allospheres at pH 6.0, a hydrodynamic diameter of 171.7 ± 14.6 nm with a signal intensity ($C(S)$) of 3.2×10^{-6} (Figure S10) was obtained when centrifugation was performed at 5000 rpm. When the rotational speed was increased to 40000 rpm for the same sample, a signal intensity of 5.1×10^{-2} was measured, indicating that 99.9% of the particle mass consisted of non-agglomerated allospheres (7.3 ± 2.9 nm; Figure S11). At 200 mg L⁻¹, similar sizes were observed, i.e. a peak intensity, $C(S)$, of 0.18 for the peak centered at 9.4 ± 2.5 nm and an intensity of 2.1×10^{-5} at 157 ± 11.9 nm (Figure S12, S13).

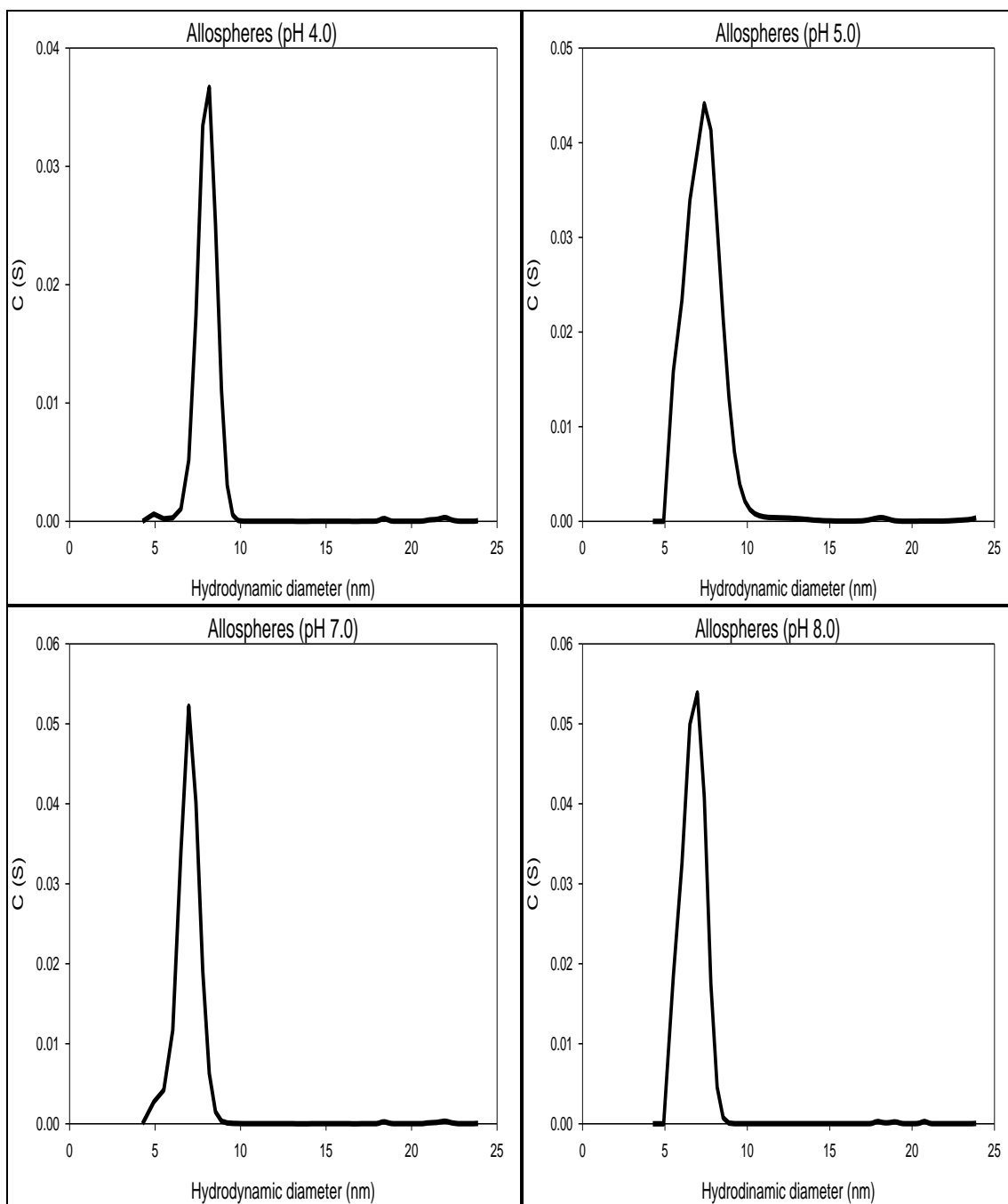


Figure S8. Hydrodynamic diameters of 5 mg L⁻¹ of the polymeric nanoparticles (allospheres) at different pH (4.0, 5.0, 7.0, 8.0) as obtained by SV-AUC using interference detection. Results for pH 6.0 are found in the body of the main paper.

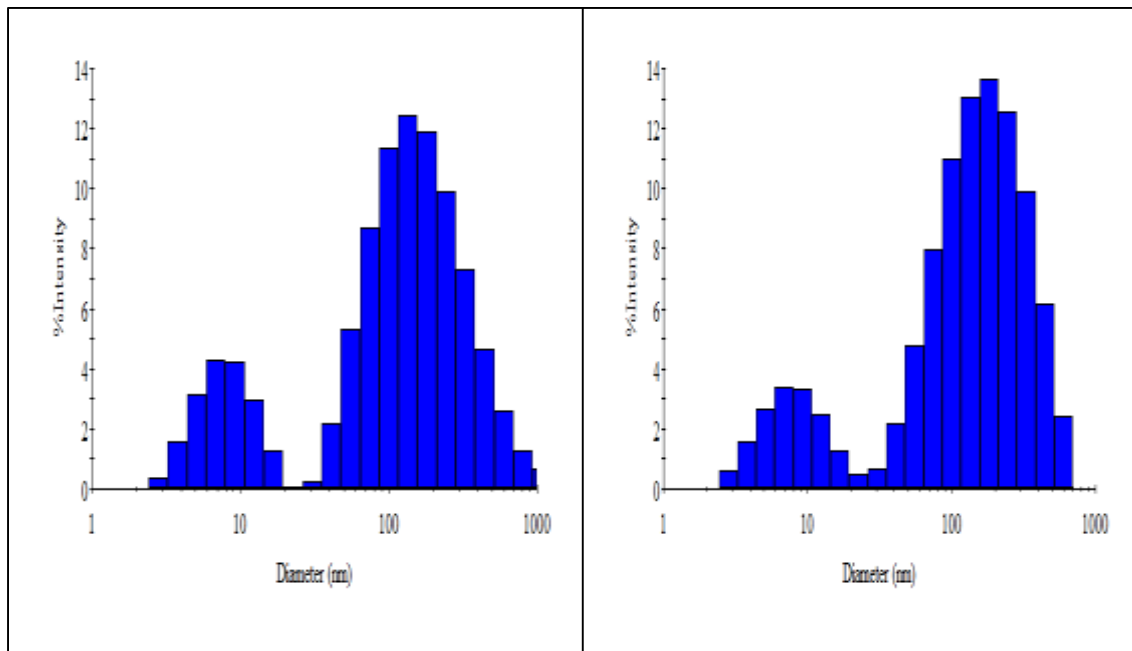


Figure S9. Hydrodynamic diameters of 200 mg L⁻¹ of the polymeric nanoparticles (allospheres) at pH 7.0 and 8.0 as obtained determined by DLS.

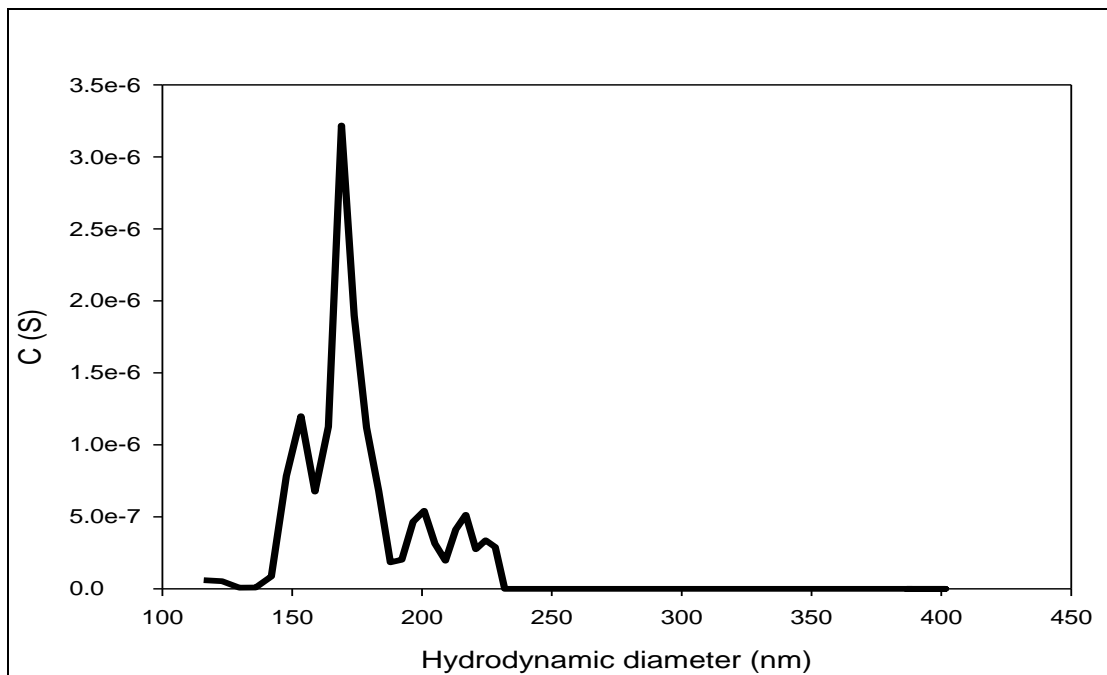


Figure S10. Hydrodynamic diameters of 5 mg L⁻¹ of the polymeric nanoparticles (allospheres) at pH 6.0 as determined by AUC (5000 rpm, RCF = 2016 x g).

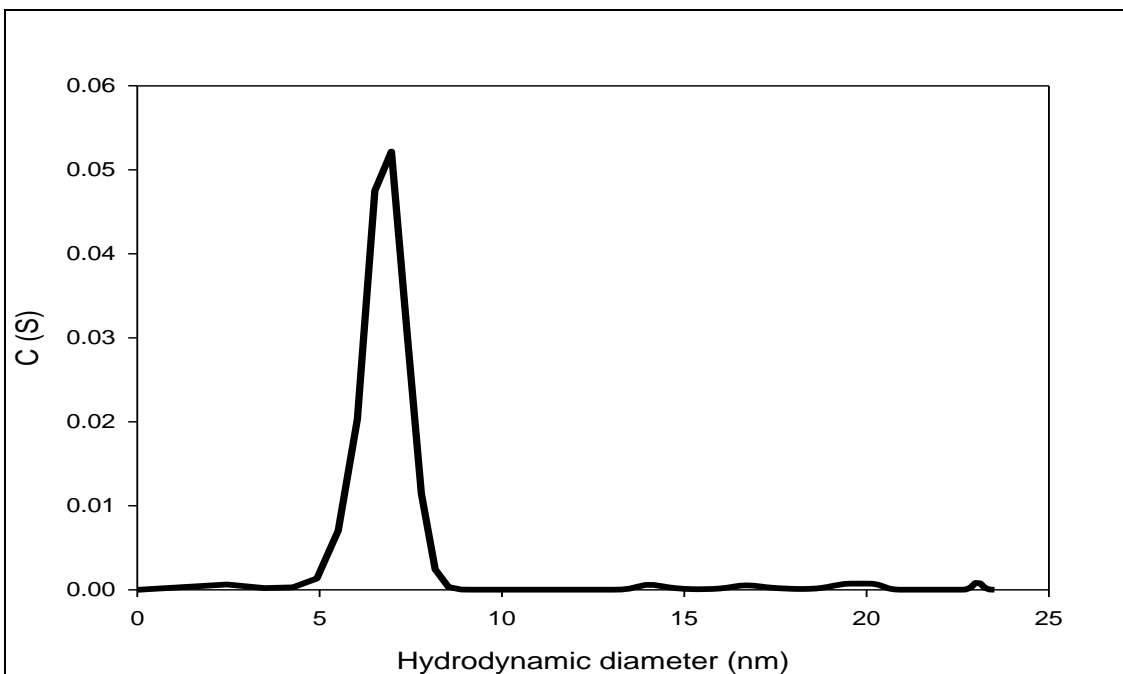


Figure S11. Hydrodynamic diameters of 5 mg L⁻¹ of the polymeric nanoparticles (allospheres) at pH 6.0 as determined by AUC (40000 rpm, RCF = 129024 x g).

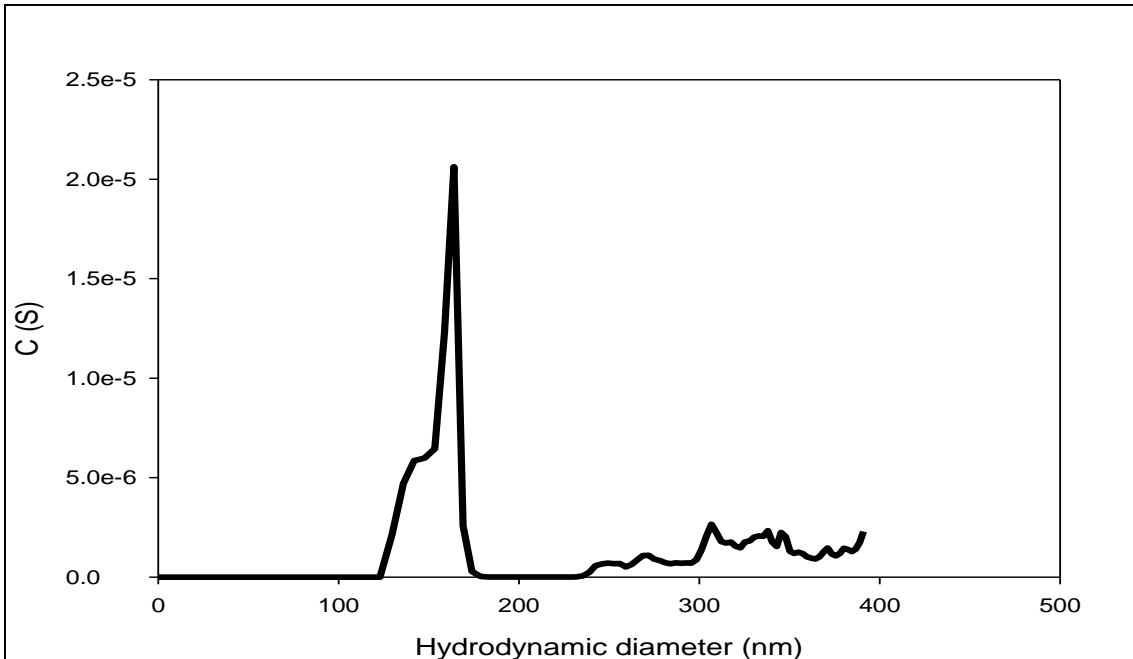


Figure S12. Hydrodynamic diameters of 200 mg L⁻¹ of the polymeric nanoparticles (allospheres) at pH 6.0 as determined by AUC (5000 rpm, RCF = 2016 x g).

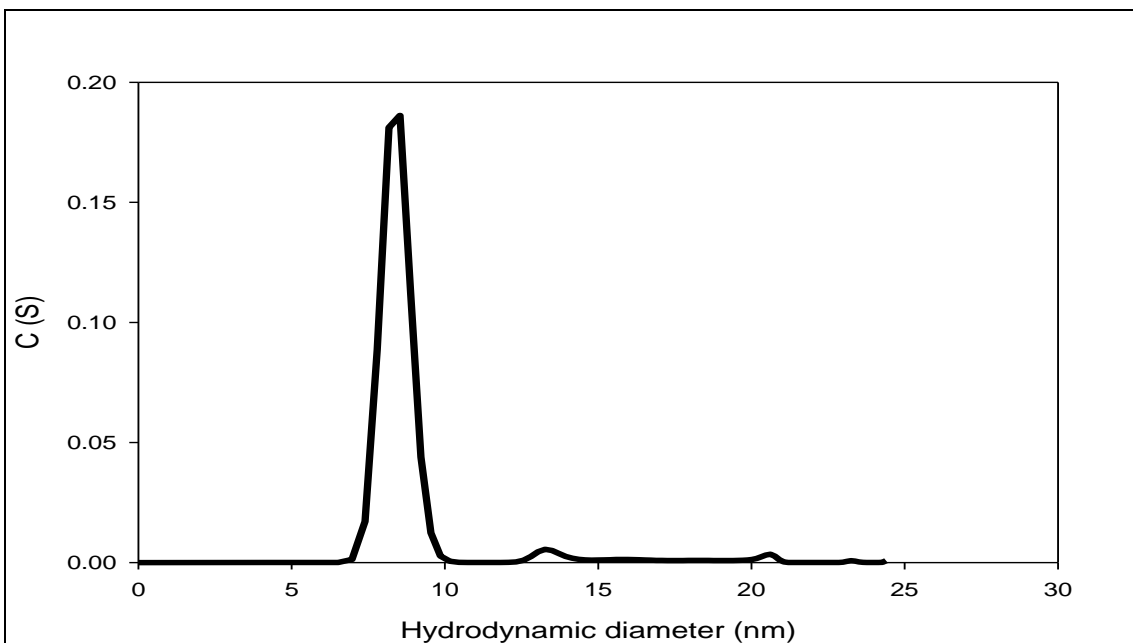


Figure S13. Hydrodynamic diameters of 200 mg L⁻¹ of the polymeric nanoparticles (allospheres) at pH 6.0 as determined by AUC (40000 rpm, RCF = 129024 x g).

S4. Size of the soil humic acid determined by fluorescence correlation spectroscopy (FCS)

The FCS technique has been described in detail elsewhere (5), and been used previously to determine the diffusion coefficients of the humic substances (6). In brief, the technique is based on the analysis of fluorescence intensity fluctuations of molecules passing through a small (ca. 1 μm^3), illuminated (Ar^+ , 488 nm) volume defined by confocal optics. Temporal fluctuations in the measured fluorescence intensity in the sample volume are used to derive an autocorrelation curve. In absence of any other processes that affect sample fluorescence, the autocorrelation curve will be related to the translational diffusion of the fluorescent sample through the confocal volume. Diffusion times of the HS are obtained from a best fit of the autocorrelation function (Eq. 1) following calibration of the sample volume using rhodamine-6G, which has a known diffusion coefficient of $4.0 \times 10^{-10} \text{ m}^2 \text{ s}^{-1}$ (4). Each data point was determined as the mean of three replicates, with run times of 120 s that were employed to reduce noise in the autocorrelation curves, mainly due to the low quantum yield of the HS. All FCS measurements were performed at 25 °C in an eight-welled, covered FCS cell.

The autocorrelation function can be described by the following equation:

$$G(\tau) = \frac{\langle \delta F(t) \times \delta F(t + \tau) \rangle}{\langle F(t) \rangle^2} \quad (1)$$

where τ is the diffusion time, t is the acquisition time, $F(t)$ is the fluorescence at time t and $\langle F(t) \rangle$ is the mean value. From the experimentally determined diffusion times through a calibrated confocal volume, it is possible to determine the diffusion coefficients, D , of the soil

humic acids. Diffusion coefficients are related to their hydrodynamic diameters via the Stokes-Einstein equation (Eq. 2), which assumes that they are spherical, hard spheres:

$$d_H = \frac{kT}{3\pi\eta D} \quad (2)$$

where d_H is the hydrodynamic diameter, k is the Boltzmann constant, T is the temperature in Kelvin, and η is the viscosity of the medium.

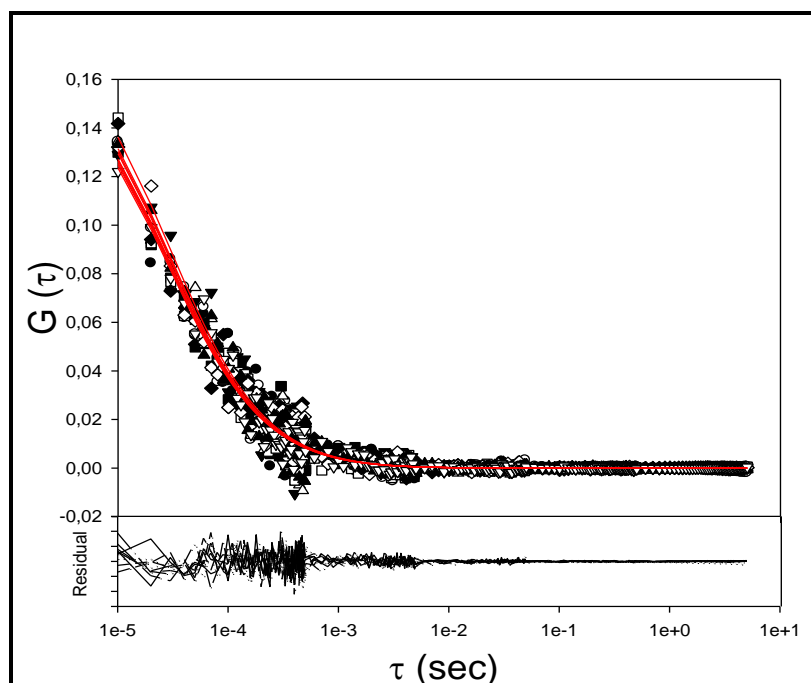


Figure. S14. Autocorrelation curve resulting from the fluorescence intensity fluctuations of 20 mg L⁻¹ of the Elliot soil humic acid.

Mean hydrodynamic diameters of 1.7 ± 0.2 nm were found for the humic acids using an excitation wavelength of 488 nm and emission bands of either 503-530 nm or 607-683 nm, in line with literature values of 2.0 nm obtained previously for a different soil humic acid (7)

S5. Composition of the natural water samples

Samples from the effluent of the Montreal wastewater treatment plant (pH 7.2) and from the Des Prairies River (pH 7.3) were collected and spiked with allospheres prior to their analysis by AUC. The major ion content of the two samples is presented in Table S4. Analysis of dissolved organic carbon (DOC) gave 7.58 and 7.38 mg C L⁻¹ for the river water and the wastewater effluent, respectively.

Table S4. Major ions in the two natural waters.

Sample ID	Na (mmol/L)	Mg (mmol/L)	K (mmol/L)	Ca (mmol/L)
Surface water	0.227 ± 0.005	0.107 ± 0.003	0.017 ± 0.002	0.164 ± 0.004
Effluent water	5.542 ± 0.289	0.828 ± 0.039	0.379 ± 0.023	0.993 ± 0.035

Bibliography

1. Nontapot K, Rastogi V, Fagan J.A, Reipa V. Size and density measurement of core-shell Si nanoparticles by analytical ultracentrifugation. *Nanotechnology*. 2013;24(15).
2. Cole J.L, Lary J.W, Moody T.P, Laue T.M. Analytical ultracentrifugation: Sedimentation velocity and sedimentation equilibrium. In: Correia JJ, Detrich HW, editors. Biophysical Tools for Biologists: Vol 1 in Vitro Techniques. *Methods in Cell Biology*. 842008. p. 143-79.
3. Peulen TO.; Wilkinson KJ. Diffusion of Nanoparticles in a Biofilm. *Environ Sci Technol*. 2011;45(8):3367-73.
4. Gendron PO.; Avaltroni F.; Wilkinson KJ. Diffusion Coefficients of Several Rhodamine Derivatives as Determined by Pulsed Field Gradient-Nuclear Magnetic Resonance and Fluorescence Correlation Spectroscopy. *J Fluoresc*. 2008;18(6):1093-101.
5. Starchev K.; Wilkinson KJ.; Buffle J. Application of FCS to the study of environmental systems. *Fluorescence Correlation Spectroscopy: Theory and Applications*. 2001;65:251-75.
6. Lead JR.; Wilkinson KJ.; Starchev K.; Canonica S, Buffle J. Determination of diffusion coefficients of humic substances by fluorescence correlation spectroscopy: Role of solution conditions. *Environ Sci Technol*. 2000;34(7):1365-9.
7. Cameron RS.; Thornton BK.; Swift RS.; Posner AM. Molecular-weight and shape of humic acid from sedimentation and diffusion measurements on fractionated extracts. *Journal of Soil Science*. 1972;23(4):394-408.